

Design and Synthesis of *N*-Substituted Indazole-3-Carboxamides as Poly(ADP-ribose)polymerase-1 (PARP-1) Inhibitors[†]

Maulik R. Patel, Kashyap G. Pandya, Cesar A. Lau-Cam, Satyakam Singh, Maria A. Pino, Blase Billack, Kurt Degenhardt and Tanaji T. Talele*

Department of Pharmaceutical Sciences, College of Pharmacy and Allied Health Professions, St. John's University, Queens, NY 11439, USA

*Corresponding author: Tanaji Talele, talelet@stjohns.edu

[†]Part of this work was presented at the 236th ACS National Meeting, Philadelphia, PA, August 17–21, 2008 and 238th ACS National Meeting, Washington DC, August 16–20, 2009.

A group of novel *N*-1-substituted indazole-3-carboxamide derivatives were synthesized and evaluated as inhibitors of poly(ADP-ribose)polymerase-1 (PARP-1). A structure-based design strategy was applied to a weakly active unsubstituted 1*H*-indazole-3-carboxamide **2, by introducing a three carbon linker between 1*H*-indazole-3-carboxamide and different heterocycles, and led to compounds **4** [1-(3-(piperidine-1-yl)propyl)-1*H*-indazole-3-carboxamide, IC₅₀ = 36 μM] and **5** [1-(3-(2,3-dioxindolin-1-yl)propyl)-1*H*-indazole-3-carboxamide, IC₅₀ = 6.8 μM]. Compound **5** was evaluated in rats for its protective action against diabetes induced by a treatment with streptozotocin, a known diabetogenic agent. In addition to preserving the ability of the pancreas to secrete insulin, compound **5** was also able to attenuate the ensuing hyperglycemic response to a significant extent.**

Key words: 2,3-dioxindoline, docking, diabetes, indazole-3-carboxamide, PARP-1

Received 21 May 2011, revised 3 December 2011 and accepted for publication 3 December 2011

Poly(ADP-ribose)polymerase-1 (PARP-1) is a chromatin-bound nuclear enzyme involved in physiological functions such as DNA replication and repair, cellular proliferation, differentiation, and apoptosis (1,2). PARP-1 is a DNA nick sensor that by signaling the presence of DNA damage facilitates DNA repair (3). In this role, this polymerase catalyzes the addition of ADP-ribose units to histones and to various DNA repair enzymes participating in replication, transcription, differentiation, gene regulation, protein degradation, and spindle maintenance (3–6).

In spite of a lack of a complete understanding of the various pathways leading to PARP-1 activation, it has, however, become apparent that the inhibition of PARP-1 with appropriate pharmacological agents may translate into protection against the development of diabetes (7–9). Numerous studies in laboratory animals, in which diabetes was induced by using diabetogenic agents such as streptozotocin (STZ) or alloxan (10–12), have suggested the possibility of using PARP-1 inhibitors as a therapeutic approach for the prevention of diabetes and its complications. For example, experimental work in rodents with two known PARP-1 inhibitors, 3-aminobenzamide (3-AB) and nicotinamide (NI), has conclusively shown that the administration of these compounds, concurrently with or shortly after STZ, can prevent the diabetogenic effects of STZ *in vivo*, as manifested by the attenuation of hyperglycemia and hypoinsulinemia and by the increase in the pancreatic synthesis and secretion of insulin (7,8). Therefore, PARP-1 inhibitors may prove beneficial in preventing or delaying the onset as well as the complications of diabetes. The purpose of this article is to describe the synthesis, structure–activity relationship (SAR) study, and *in vitro* and *in vivo* evaluation of *N*-1-substituted indazole-3-carboxamide derivatives as PARP-1 inhibitors and antidiabetogenic agents.

Molecular Design

Initial *in vitro* evaluation of 1*H*-indazole-3-carboxamide (**2**) as a PARP-1 inhibitor indicated this compound to exhibit only a modest (25% inhibition at 50 μM) activity. In the structure of **2**, the N₂ atom of the indazole core may lock the carboxamide group into the desired conformation by an intramolecular hydrogen bond to form a pseudotricyclic (6:5:5) ring system, whereas the R group may be able to gain access to the adenosine (AD)-binding site of PARP-1 (Figure 1). Starting with compound **2** as a NI-mimic, we set out to investigate the possibility of enhancing the PARP-1 inhibitory activity by structurally modifying this scaffold at the *N*-1 position by altering heterocyclic ring at the terminal carbon atom of the propyl linker. To attain this goal, a molecular docking study was carried out using the X-ray crystal structure of the C-terminal catalytic fragment of human PARP-1 (pdb ID: 2rcw) in complex with 2-substituted benzimidazole-4-carboxamide inhibitor. Compound **2** was docked into the catalytic site of human PARP-1 (Figure 2) using GLIDE DOCKING program v5.0 (Schrodinger LLC, New York, NY, USA). The widely accepted consensus pharmacophore for inhibition of PARP-1 (13), developed by classical SAR studies and by modeling using the X-ray crystal structure of the catalytic (NAD⁺-binding) domain (14,15), is a primary or secondary benzamide, which makes important hydro-

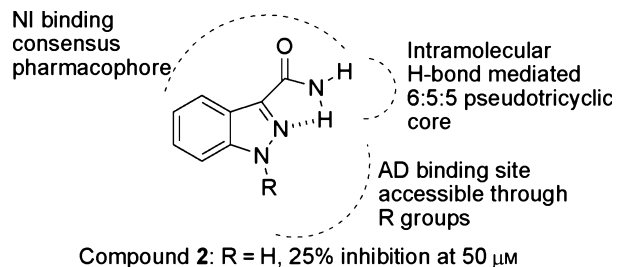


Figure 1: Development of new class of indazole-3-carboxamide poly(ADP-ribose)polymerase-1 inhibitors.

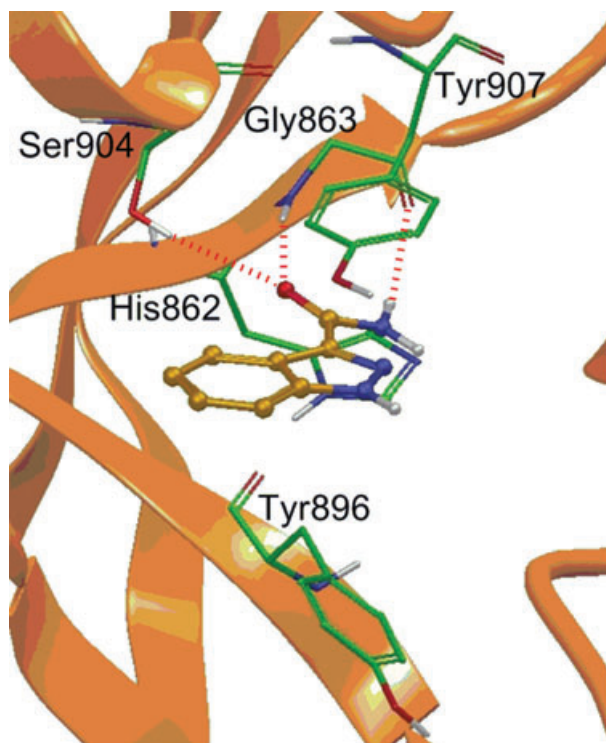


Figure 2: Standard precision-Glide predicted binding pose for compound 2 within the active site of poly(ADP-ribose)polymerase-1. Important amino acids are depicted as sticks with the atoms colored as carbon – green, hydrogen – white, nitrogen – blue, and oxygen – red, whereas the inhibitor is shown as ball and stick model with the same color scheme as above except carbon atoms are represented in orange. Dotted red lines indicate hydrogen bonding interaction.

gen bonds with Gly863 (-NH to Gly -C=O and -C=O to Gly -NH) and Ser904 (-C=O to Ser -OH) in addition to π -stacking with Tyr907 and, to some extent, with Tyr896 in the PARP-1 enzyme. In agreement with the aforementioned findings, compound 2 bound to the NI site by a sandwiched hydrophobic interaction with the phenyl rings of Tyr896 and Tyr907 and the imidazole ring of His862. The amide group formed a total of three hydrogen bonds represented by (-C=O—HO- Ser904), (-C=O—HN- Gly863), and (-NH—O=C- Gly863). On the basis of the molecular docking of compound 2, it was possible to verify that the *N*-1 position offered an open pocket that

could accommodate heteroaryl alkyl chains amenable for the investigation of SAR. Using this line of reasoning, *N*-1-substituted derivatives were synthesized and evaluated *in vitro* for inhibitory activity toward PARP-1 and, more importantly, for singling out an analog with a demonstrable high potency to prevent the development of glucose intolerance in an animal model of diabetes.

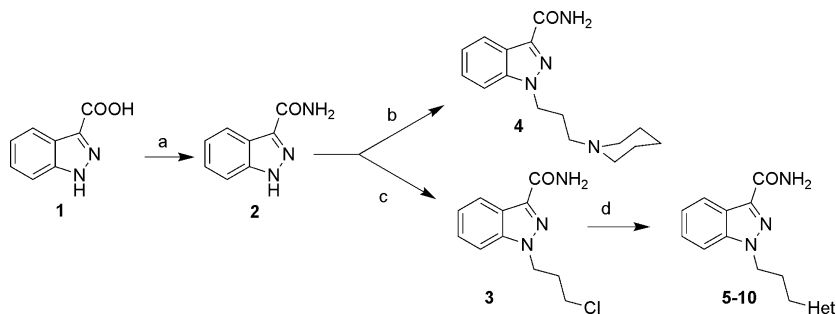
Chemistry

The synthesis of 1*H*-indazole-3-carboxamide and its derivatives is depicted in Scheme 1. Compound 2 was obtained by treating compound 1 with isobutyl chloroformate and *N*-methylmorpholine (NMM) in THF followed by *in situ* addition of 30% aqueous ammonia. Alkylation of compound 2 with 1-bromo-3-chloropropane under basic condition provided compound 3. The selective alkylation of the *N*-1 position remains a challenge, specifically for C_3 -unsubstituted indazoles (16). It has been previously reported that use of potassium carbonate as a base yielded 92:1 ratio of *N*-1 versus *N*-2-alkylated indazole derivatives (17). Moreover, the portion of *N*-2-alkylated products is highly dependent on the bulkiness of the substituent at C_3 position as exemplified through *N*-1 versus *N*-2 ratio of 65:35 (when C_3 =-H) as opposed to the corresponding ratio of 95:5 (when C_3 =4-fluorophenyl) (18). On the basis of these prior findings, we anticipated the formation of compound 3 (*N*-1 regioisomer) as the major product. Compound 3 was assigned as *N*-1 regioisomer based on ^{13}C NMR and 1D NOE spectral data. First, structural assignment of compound 3 as the *N*-1 regioisomer was observed in the ^{13}C NMR spectra, where the resonance of C_3 of the indazole ring was downfield (δ 140.7 ppm) and the resonance of C_{7a} of the indazole ring was upfield (δ 137.5 ppm) in agreement with the previously reported values for *N*-1-substituted indazole derivatives (18–20). Second evidence for the structural assignment of compound 3 was obtained by a 1D NOE experiment. Irradiation of the signal for the 1'- CH_2 -protons (triplet at δ 4.59 ppm) resulted in a 4.7% enhancement of the signal for the H_7 proton (doublet at δ 7.74 ppm) without any enhancement for the amide proton signals (two singlet at δ 7.69 and 7.40 ppm) (Supplementary data, Figure S1). These data clearly indicate that 1'- CH_2 - and the C_7 -hydrogen are in close proximity to each other (Figure 3). Analysis of the ^{13}C NMR and 1D NOE spectral data of compound 5 was found to be in agreement with the aforementioned findings (Supplementary data, Figure S2). Taken together, the ^{13}C NMR and 1D NOE spectral data described clearly support the structural assignment made. Target compound 4 was prepared by direct alkylation of compound 2 with commercially available 3-chloropropylpiperidine-1-yl. Target compounds 5–10 were prepared by reacting compound 3 with the corresponding heterocycles under basic condition.

Materials and Methods

Chemistry

Melting points (mp) were determined on a Thomas-Hoover capillary melting point apparatus and are uncorrected. Reagents for organic synthesis were purchased from Aldrich Chemical Co. (Milwaukee, WI, USA), TCI America (Portland, OR, USA), Alfa Aesar (Ward Hill, MA, USA), and Acros Organics (Antwerp, Belgium) and were used



Scheme 1: (a) *i*-BuOCCl, NMM, THF, -20°C , 2 h; NH_4OH (30%), rt, 1 h, 85%; (b) K_2CO_3 , 3-chloropropylpiperidin-1-yl, CH_3CN , reflux, 4 h, 75%; (c) K_2CO_3 , 1-bromo-3-chloropropane, CH_3CN , reflux, 4 h, 62%; (d) K_2CO_3 , Heterocycle (Het), CH_3CN , reflux, 4 h, 34–70%.

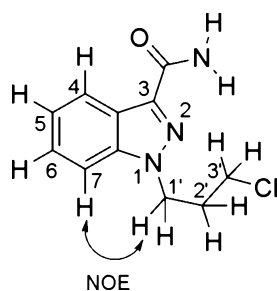


Figure 3: The NOE detected for compound **3**.

as received. All compounds were checked for homogeneity by TLC using silica gel as a stationary phase. The ^1H NMR spectra were recorded on a Bruker 400 Avance DPX spectrometer outfitted with a z -axis gradient probe. The chemical shifts are reported as parts per million (δ ppm) downfield from tetramethylsilane (TMS) as an internal standard. Data are reported as follows: chemical shift, multiplicity (s) singlet, (d) doublet, (t) triplet, (qn) quintet, (m) multiplet, (dd) doublet of doublet, and (bs) broad singlet. 1D-NOESY spectra were processed with pulse width of 60 ms, power level of 64.7 dB, phase correlation of 10.0, and 0.3 Hz line broadening. The C, H, and N analyses were performed by Atlantic Microlabs, Inc., (Norcross, GA, USA), and the observed values were within $\pm 0.4\%$ of calculated values.

1*H*-Indazole-3-carboxamide (**2**)

To a solution of indazole 3-carboxylic acid **1** (0.30 g, 1.85 mmol) in anhydrous THF (7 mL) was added isobutyl chloroformate (0.28 g, 2.04 mmol) and NMM (0.21 g, 2.04 mmol) under a nitrogen atmosphere and -20°C , and the mixture was stirred for 2 h. Then, to this mixture, 5 mL of aqueous NH_3 (30%) was added and the mixture was stirred at rt for 1 h. The mixture was then diluted with EtOAc (5 mL), partitioned with water (2×10 mL), dried over Na_2SO_4 , and concentrated in vacuum. Following purification of the residue by column chromatography using $\text{CH}_2\text{Cl}_2/\text{MeOH}$ (95:5) as the eluent, the product was obtained as white crystals (0.25 g, 85%); m.p. $284\text{--}286^{\circ}\text{C}$ (lit. $285\text{--}286^{\circ}\text{C}$) (21); ^1H NMR (400 MHz, DMSO-d_6 , TMS) δ 13.57 (s, 1H), 8.17 (d, 1H, $J = 7.8$ Hz), 7.76 (s, 1H), 7.60 (d, 1H, $J = 8.4$ Hz), 7.40 (t, 1H, $J = 7.6$ Hz), 7.36 (s, 1H), 7.23 (t, 1H, $J = 7.2$ Hz); ^{13}C NMR (100 MHz, DMSO-d_6 , TMS) δ 164.5, 141.2, 138.4, 126.5, 122.1, 121.8, 121.7, 110.7; Anal. Calcd.

for $\text{C}_8\text{H}_7\text{N}_3\text{O}$: C, 59.62; H, 4.38; N, 26.07. Found C, 59.43; H, 4.19; N, 25.82.

N-(3-Chloropropyl)-1*H*-indazole-3-carboxamide (**3**)

To a suspension of compound **2** (0.300 g, 1.86 mmol) in CH_3CN (10 mL), 1-bromo-3-chloropropane (0.321 g, 2.046 mmol) and anhydrous K_2CO_3 (0.564 g, 4.09 mmol) were added in succession, and the mixture was stirred under reflux for 4 h. The mixture was then filtered and concentrated under vacuum. The resulting solid was purified by column chromatography (EtOAc:Hexane 60:40) to yield the product as a white solid (0.286 g, 62%); m.p. $108\text{--}112^{\circ}\text{C}$; ^1H NMR (400 MHz, DMSO-d_6 , TMS) δ 8.18 (d, 1H, $J = 8.4$ Hz), 7.74 (d, 1H, $J = 8.0$ Hz), 7.69 (s, 1H), 7.46 (t, 1H, $J = 7.7$ Hz), 7.40 (s, 1H), 7.26 (t, 1H, $J = 7.5$ Hz), 4.59 (t, 2H, $J = 6.6$ Hz), 3.65 (t, 2H, $J = 6.2$ Hz), 2.33 (qn, 2H, $J = 6.4$ Hz); ^{13}C NMR (100 MHz, DMSO-d_6 , TMS) δ 163.8, 140.7, 137.5, 126.6, 122.4, 122.3, 122.0, 110.1, 45.8, 42.4, 32.2.

1-(3-(Piperidin-1-yl)propyl)-1*H*-indazole-3-carboxamide (**4**)

This compound was synthesized by the procedure used for compound **3**, by alkylating compound **2** (0.150 g, 0.932 mmol) with *N*-(3-chloropropyl)piperidine (0.164 g, 1.01 mmol) to yield compound **4** as a pale yellow solid (0.160 g, 59%); m.p. $92\text{--}94^{\circ}\text{C}$; ^1H NMR (400 MHz, DMSO-d_6 , TMS) δ 8.16 (d, 1H, $J = 8.4$ Hz), 7.73 (d, 1H, $J = 8.4$ Hz), 7.66 (s, 1H), 7.42 (t, 1H, $J = 7.4$ Hz), 7.37 (s, 1H), 7.23 (t, 1H, $J = 7.4$ Hz), 4.47 (t, 2H, $J = 6.5$ Hz), 2.15 (m, 6H), 2.00 (qn, 2H, $J = 6.7$ Hz), 1.44 (qn, 4H, $J = 5.4$ Hz), 1.34 (qn, 2H, $J = 5.2$ Hz); ^{13}C NMR (100 MHz, DMSO-d_6 , TMS) δ 164.0, 140.8, 137.2, 126.2, 122.2 (2C), 121.8, 110.4, 55.2, 53.9 (2C), 46.6, 26.6, 25.5 (2C), 24.1; Anal. Calcd. for $\text{C}_{16}\text{H}_{22}\text{O}_1\text{N}_4$: C, 67.13; H, 7.69; N, 19.58. Found: C, 66.89; H, 7.75; N, 19.28.

1-(3-(2,3-Dioxindolin-1-yl)propyl)-1*H*-indazole-3-carboxamide (**5**)

This compound was synthesized by the procedure used for compound **3**, by alkylating 2,3-dioxindoline (0.100 g, 0.680 mmol) with the halide intermediate **3** (0.162 g, 0.680 mmol) to yield compound **5** as a brick-red solid (0.165 g, 70%); m.p. $186\text{--}188^{\circ}\text{C}$; ^1H NMR

(400 MHz, DMSO- d_6 , TMS) δ 8.19 (d, 1H, J = 8.6 Hz), 7.78 (d, 1H, J = 8.6 Hz), 7.68 (s, 1H), 7.61 (t, 1H, J = 7.8 Hz), 7.54 (d, 1H, J = 7.2 Hz), 7.44 (m, 2H), 7.27 (t, 1H, J = 7.2 Hz), 7.13 (m, 2H), 4.59 (t, 2H, J = 6.7 Hz), 3.76 (t, 2H, J = 6.7 Hz), 2.28 (qn, 2H, J = 6.9 Hz); ^{13}C NMR (100 MHz, DMSO- d_6 , TMS) δ 183.3, 163.8, 158.2, 150.4, 139.6, 137.9, 137.3, 126.4, 124.3, 123.0, 122.3, 122.1, 121.9, 117.6, 110.5, 110.3, 46.2, 37.2, 26.9; Anal. Calcd. for $\text{C}_{19}\text{H}_{16}\text{O}_3\text{N}_4 \cdot \frac{1}{4} \text{CH}_3\text{OH}$: C, 66.37; H, 4.89; N, 16.09. Found: C, 66.15; H, 4.73; N, 16.24.

1-(3-(5-Fluoro-2,3-dioxindolin-1-yl)propyl)-1H-indazole-3-carboxamide (6)

This compound was synthesized by the procedure used for compound **3**, by alkylating 5-fluoro-2,3-dioxindoline (0.100 g, 0.606 mmol) with halide intermediate **3** (0.144 g, 0.606 mmol) to yield compound **6** as an orange-red solid (0.076 g, 34%); m.p. 184–187 °C; ^1H NMR (400 MHz, DMSO- d_6 , TMS) δ 8.15 (d, 1H, J = 8.4 Hz), 7.75 (d, 1H, J = 8.4 Hz), 7.62 (s, 1H), 7.44 (m, 4H), 7.25 (t, 1H, J = 7.8 Hz), 7.17 (dd, 1H, J = 8.6 Hz, 5.0 Hz), 4.56 (t, 2H, J = 6.8 Hz), 3.77 (t, 2H, J = 6.8 Hz), 2.25 (qn, 2H, J = 6.6 Hz); ^{13}C NMR (100 MHz, DMSO- d_6 , TMS) δ 182.6, 163.8, 159.6, 157.2, 146.6, 140.6, 137.3, 126.4, 123.9, 123.6, 122.3, 122.1, 121.9, 118.6, 111.9, 110.3, 46.1, 37.3, 26.7; Anal. Calcd. for $\text{C}_{19}\text{H}_{15}\text{O}_3\text{N}_4\text{F} \cdot \frac{1}{3} \text{EtOAc}$: C, 61.72; H, 4.50; N, 14.16. Found: C, 61.63; H, 4.35; N, 14.34.

1-(3-(5-Chloro-2,3-dioxindolin-1-yl)propyl)-1H-indazole-3-carboxamide (7)

This compound was synthesized by the procedure used for compound **3**, by alkylating 5-chloro-2,3-dioxindoline (0.100 g, 0.552 mmol) with halide intermediate **3** (0.131 g, 0.552 mmol) to yield compound **7** as an orange solid (0.094 g, 44%); m.p. 195–197 °C; ^1H NMR (400 MHz, DMSO- d_6 , TMS) δ 8.15 (d, 1H, J = 7.7 Hz), 7.75 (d, 1H, J = 8.6 Hz), 7.62 (m, 3H), 7.41 (m, 2H), 7.24 (t, 1H, J = 7.8 Hz), 7.18 (d, 1H, J = 8.2 Hz), 4.56 (t, 2H, J = 7.2 Hz), 3.77 (t, 2H, J = 6.6 Hz), 2.25 (qn, 2H, J = 6.8 Hz); ^{13}C NMR (100 MHz, DMSO- d_6 , TMS) δ 182.2, 163.8, 158.0, 148.9, 140.6, 137.3, 136.7, 127.3, 126.4, 123.8, 122.3, 122.1, 121.9, 119.1, 112.3, 110.4, 46.1, 37.3, 26.7; Anal. Calcd. for $\text{C}_{19}\text{H}_{15}\text{O}_3\text{N}_4\text{Cl}$: C, 59.61; H, 3.95; N, 14.04. Found: C, 59.43; H, 3.71; N, 14.24.

1-(3-(5-Bromo-2,3-dioxindolin-1-yl)propyl)-1H-indazole-3-carboxamide (8)

This compound was synthesized by the procedure used for compound **3**, by alkylating 5-bromo-2,3-dioxindoline (0.100 g, 0.442 mmol) with halide intermediate compound **3** (0.105 g, 0.442 mmol) to yield compound **8** as a dark orange solid (0.092 g, 49%); m.p. 204–206 °C; ^1H NMR (400 MHz, DMSO- d_6 , TMS) δ 8.15 (d, 1H, J = 8.0 Hz), 7.75 (m, 2H), 7.68 (d, 1H, J = 2.4 Hz), 7.62 (s, 1H), 7.42 (m, 2H), 7.25 (t, 1H, J = 7.4 Hz), 7.13 (d, 1H, J = 8.0 Hz), 4.56 (t, 2H, J = 7.0 Hz), 3.76 (t, 2H, J = 7.0 Hz), 2.24 (qn, 2H, J = 6.8 Hz); ^{13}C NMR (100 MHz, DMSO- d_6 , TMS) δ 182.0, 163.8, 157.9, 149.3, 140.5, 139.5, 137.3, 126.6, 126.5, 122.3, 122.2, 121.9, 119.4, 114.8, 112.7, 110.4, 46.1, 37.3, 26.7; Anal. Calcd. for

$\text{C}_{19}\text{H}_{15}\text{O}_3\text{N}_4\text{Br} \cdot \frac{1}{3} \text{EtOAc}$: C, 53.48; H, 3.90; N, 12.27. Found: C, 53.23; H, 3.68; N, 12.47.

1-(3-(5-Iodo-2,3-dioxindolin-1-yl)propyl)-1H-indazole-3-carboxamide (9)

This compound was synthesized by the procedure used for compound **3**, by alkylating 5-iodo-2,3-dioxindoline (0.150 g, 0.549 mmol) with halide intermediate **3** (0.130 g, 0.549 mmol) to yield compound **9** as an orange solid (0.127 g, 49%); m.p. 212–214 °C; ^1H NMR (400 MHz, DMSO- d_6 , TMS) δ 8.15 (d, 1H, J = 8.0 Hz), 7.90 (d, 1H, J = 8.6 Hz), 7.78 (s, 1H), 7.75 (d, 1H, J = 8.0 Hz), 7.61 (s, 1H), 7.42 (m, 2H), 7.25 (t, 1H, J = 8.0 Hz), 7.00 (d, 1H, J = 7.6 Hz), 4.55 (t, 2H, J = 6.8 Hz), 3.75 (t, 2H, J = 7.4 Hz), 2.24 (qn, 2H, J = 6.6 Hz); ^{13}C NMR (100 MHz, DMSO- d_6 , TMS) δ 182.0, 163.8, 157.6, 149.7, 145.3, 140.6, 140.2, 137.3, 132.0, 126.5, 122.3, 122.2, 121.9, 119.7, 113.0, 110.3, 46.1, 37.3, 26.7; Anal. Calcd. for $\text{C}_{19}\text{H}_{15}\text{O}_3\text{N}_4\text{I} \cdot \frac{1}{6} \text{EtOAc}$: C, 48.31; H, 3.37; N, 11.46. Found: C, 48.04; H, 3.68; N, 11.08.

1-(3-(5-Methoxy-2,3-dioxindolin-1-yl)propyl)-1H-indazole-3-carboxamide (10)

This compound was synthesized by the procedure used for compound **3**, by alkylating 5-methoxy-2,3-dioxindoline (0.100 g, 0.565 mmol) with halide intermediate **3** (0.134 g, 0.565 mmol) to yield compound **10** as a dark brown solid (0.090 g, 42%); m.p. 161–163 °C; ^1H NMR (400 MHz, DMSO- d_6 , TMS) δ 8.15 (d, 1H, J = 8.6 Hz), 7.75 (d, 1H, J = 8.6 Hz), 7.63 (s, 1H), 7.42 (m, 2H), 7.24 (t, 1H, J = 7.6 Hz), 7.18 (dd, 1H, J = 8.4 Hz, 3.0 Hz), 7.11 (d, 1H, J = 3.0 Hz), 7.07 (d, 1H, J = 8.0 Hz), 4.56 (t, 2H, J = 7.4 Hz), 3.75 (m, 5H), 2.24 (qn, 2H, J = 7.4 Hz); ^{13}C NMR (100 MHz, DMSO- d_6 , TMS) δ 183.5, 163.8, 158.2, 155.6, 144.2, 140.6, 137.2, 126.4, 123.6, 122.3, 122.2, 121.9, 118.2, 111.6, 110.3, 109.2, 55.9, 46.2, 37.2, 26.9; Anal. Calcd. for $\text{C}_{20}\text{H}_{18}\text{O}_4\text{N}_4$: C, 63.49; H, 4.79; N, 14.81. Found: C, 63.62; H, 4.79; N, 14.71.

PARP-1 inhibition assay

Inhibitory action of the various indazole-3-carboxamide derivatives toward PARP-1 was determined using a commercially available microplate assay kit (Catalog # 4677-096-K; Universal Colorimetric PARP Assay from Trevigen, Inc., Gaithersburg, MD, USA) and according to the instructions provided by the manufacturer. Stock solutions of the various test compounds were made in dimethyl sulfoxide (DMSO), which were then serially diluted to the required concentrations with distilled water. For the assay, each strip well was filled with 10 μL of the inhibitor solution, 15 μL of diluted PARP-1 enzyme (providing 0.5 Unit/well), and 25 μL of PARP Cocktail (consisting of biotinylated NAD, activated DNA in Tris-Cl pH 8.0, and EDTA). The strip wells were incubated at room temperature for 60 min and then washed 4 times with phosphate-buffered saline (PBS: Na_2HPO_4 , NaH_2PO_4 , and NaCl) and 0.1% Triton. Then, 50 μL of diluted Strep-HRP (blocking solution) was added to each well, and the strips were further incubated at room temperature for 60 min. After washing the wells 4 times each with PBS and 0.1% Triton, they were mixed with 50 μL of TACS-Sapphire™ colorimetric substrate and allowed to stand in the dark for 10–15 min. The

intensity of the blue color that developed in each well was read on a microplate reader set at 630 nm. After stopping the reaction by the addition of 50 μ L of 5% phosphoric acid to each well, the absorbance of the yellow color was measured at 450 nm. Parallel experiments were conducted by substituting the test solution with an equivalent volume of DMSO or distilled water to verify the effect of the vehicles on the enzyme activity. All the samples were tested in triplicate. Those compounds found to inhibit PARP-1 activity by $\geq 50\%$ at a concentration of 50 μ M were further tested using various concentrations to obtain dose–response curves. To determine the IC_{50} value for each inhibitor, the average absorbance of each inhibitor concentration was plotted against the log of the concentration of each respective inhibitor (semi-log plot) and the IC_{50} value for each plot was obtained using Regression Wizard from SIGMA PLOT version 10.0 (Systat, San Jose, CA, USA). Data presented are the results of at least two independent experiments carried out in triplicate. The results of these studies are presented as mean \pm standard deviation (SD).

In vivo assessment of antidiabetic action

Animals

All the experiments were carried out on male Sprague-Dawley rats, 200–225 g in weight, obtained from Taconic Farms, Germantown, NY, USA. The animals were housed in a room maintained at a temperature of 21 ± 3 °C, a constant humidity, and a normal 12-h light/12-h dark cycle and allowed to acclimate to their new surroundings for a period of 5 days before the start of an experiment. During that time, the animals had free access to a commercial animal diet and filtered tap water. All experimental groups consisted of six animals each and they were used in a non-fasted state. The study received the approval of the Institutional Care and Use Committee of St. John's University, and the animals were cared in accordance with the guidelines established by the United States Department of Agriculture.

Treatment solutions and dosing

Solutions of the treatment compounds were prepared in either citrate buffer pH 4.5 (STZ; 3-AB) or DMSO (compound **5**) just prior to an experiment. These solutions were administered by the intraperitoneal (i.p.) route, using a 2-mL plastic syringe fitted with a 25-gauge needle, and in a volume not exceeding 2 mL. Control animals received only physiological saline, citrate buffer pH 4.5, or DMSO in a volume equal to that of a test compound. Diabetes was induced with a single, 60 mg/kg, dose of STZ, and its occurrence was ascertained by measuring the blood glucose twice, once in a drop of tail vein blood at 24-hr post-STZ and once in a blood sample collected following decapitation of the animals. In experiments in which 3-AB or compound **5** were used, these agents were administered by the i.p. route at a dose of 0.7, 1.4, and 2.1 mm/kg/2 mL at 45 min before a treatment with STZ.

Blood sample collections

The animals were killed by decapitation at 24-hr post-STZ, and their blood samples were delivered to heparinized 10-mL stoppered poly-

ethylene tubes. Plasma samples were obtained by centrifugation of the blood samples at $5193 \times g$ for 10 min, and decanting the clear supernatants into clean 10-mL polyethylene tubes. The plasma samples were kept at 4 °C in a refrigerator until needed for an assay.

Assays

Blood glucose was measured in a drop of tail vein blood using a commercial glucometer (ACCU-CHEK® Active and diabetes test strips; Roche Diagnostics Corporation U.S., Indianapolis, IN, USA). Plasma glucose was measured using a commercial enzymatic glucose assay kit (Procedure No. 510, Sigma-Aldrich, St. Louis, MO). Plasma insulin was measured using a commercially available insulin ELISA immunoassay kit (Calbiotech, Inc., Spring Valley, CA, USA).

Statistical analysis

The results are expressed as the mean \pm SEM for $n = 6$ rats. Statistical differences from control groups were established by Student's *t*-test, one-way analysis of variance, and Newman–Keuls post hoc test. A difference was considered to be statistically significant at $p \leq 0.05$.

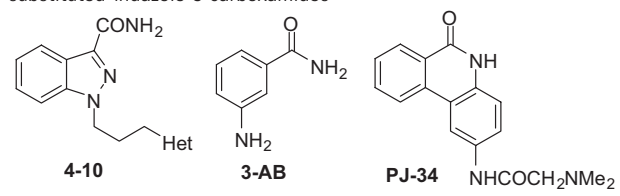
Molecular modeling

Molecular docking computations were carried out on a Dell Precision 470n workstation with the RHEL 4.0 operating system using GLIDE 5.0 (Schrodinger, LLC). 3D Structures of compounds **2** and **5** were constructed using the fragment dictionary of MAESTRO 9.0 (Schrodinger, LLC), and geometry was optimized by MacroModel program v9.5 using the OPLS-AA force field (22) with the steepest descent followed by truncated Newton conjugate gradient protocol. The X-ray crystal structure of PARP-1 in complex with 2-substituted benzimidazole-4-carboxamide inhibitor (PDB ID: 2rcw), obtained from the RCSB Protein Data Bank (PDB), was used in this study. The protein was optimized for docking using the 'Protein Preparation Wizard' and 'Prime-Refinement Utility' of MAESTRO 9.0.

Because the consensus pharmacophore for the inhibition of PARP-1 is a primary or secondary amide that makes important hydrogen bonds with Gly863 and Ser904, the grid was centered manually around the benzimidazole-4-carboxamide bound inhibitor; using the amino group of amide moiety as hydrogen bond donor and backbone carbonyl oxygen atom of Gly863 as hydrogen bond acceptor to guide the amide group of compounds **2** and **5** toward the backbone of Gly863. Then, compounds **2** and **5** were docked into the PARP-1 active site with aforementioned constraints using the standard precision Glide docking method. The top scoring pose-PARP-1 complex was then subjected to energy minimization using MACROMODEL program v9.5 using the OPLS-AA force field (22) and used for graphical analysis.

Results and Discussion

The newly synthesized indazole-3-carboxamide derivatives were tested *in vitro* for their PARP-1 inhibitory activity, results of which are presented in Table 1. The benchmark PARP-1 inhibitors 3-AB

Table 1: Poly(ADP-ribose)polymerase-1 inhibition data for *N*-1 substituted indazole-3-carboxamides


Compound	Het	IC ₅₀ , μM ^a
4	Piperidin-1-yl	36.00 ± 2.00
5	2,3-dioxindolin-1-yl	6.80 ± 0.57
6	5-fluoro-2,3-dioxindolin-1-yl	34.59 ± 1.26
7	5-chloro-2,3-dioxindolin-1-yl	41.77 ± 1.24
8	5-bromo-2,3-dioxindolin-1-yl	118.85 ± 1.91
9	5-iodo-2,3-dioxindolin-1-yl	179.76 ± 2.74
10	5-methoxy-2,3-dioxindolin-1-yl	90.21 ± 4.40
3-AB		11.00
PJ-34		0.11

^aIC₅₀ values were determined by at least two independent experiments, each carried out in triplicate.

(23,24) and PJ-34 ([2-(dimethylamino)-*N*-(6-oxo-5,6-dihydrophenanthridin-2-yl)acetamide]) (25) are included for comparison. Attachment of a piperidine-1-propyl substituent at the *N*-1 position of compound **2** resulted in compound **4** (IC₅₀ = 36 μM), a more potent inhibitor of PARP-1 than compound **2**. Analysis of the PARP-1 active site suggested availability of a large pocket that could accommodate bicyclic heterocycles capable of forming hydrogen bonding interactions with active site residues and/or water molecules. To test this concept, we have replaced the piperidine ring of compound **4** with a 2,3-dioxindoline moiety, which provided compound **5** (IC₅₀ = 6.8 μM) with >5-fold improvement in potency relative to compound **4**.

Having established that the 2,3-dioxindoline ring being optimum for PARP-1 inhibitory activity when inserted at the terminal carbon atom of the linker, we decided to examine the effect of introducing a shorter (ethyl) and longer (butyl) linker on the PARP-1 inhibitory activity of compound **5**. To this end, 2,3-dioxindoline analogs with two (compound **S-2**) and four (compound **S-4**) carbon linkers between the indazole-3-carboxamide and 2,3-dioxindoline were synthesized, tested, and proved to be significantly less active than compound **5** (Supplementary data, Table S1). At this point, further activity optimization efforts on 2,3-dioxindoline derivatives were directed at examining the effect of relocating the hydrogen bond acceptor groups of the 2,3-dioxindoline moiety of compound **5** as well as of steric bulkiness. On this basis, a 1,3-dioxoisindoline analog (compound **S-5**) was synthesized and tested but found to be significantly less potent than compound **5**. Further removal of the phenyl portion of the 1,3-dioxoisindoline moiety resulted in pyrrolidine-2,5-dione analog **S-6**, which also proved to be inferior than compound **5**. Next, we focused our attention to replace the propyl linker with 2-propanol (compound **S-8**) and propanoyl (compound **S-10**) linkers; however, both of these compounds showed 5- to 6-fold less activity than compound **5** (Supplementary data, Table S1).

To establish the role of the phenyl portion of the 2,3-dioxindoline moiety in compound **5** toward PARP-1 inhibition, a short series of 5-substituted 2,3-dioxindoline analogs were synthesized and subjected to *in vitro* testing for PARP-1 inhibitory potency. From the IC₅₀ values shown in Table 1, it was possible to rank the PARP-1 inhibitory activity of the compounds in this series in the decreasing order H>>F>Cl>>OMe>Br>>I. Thus, any substitution on the 2,3-dioxindoline aryl ring appears to be detrimental to the PARP-1 inhibitory action for reasons that are not clear at present. On the basis of the aforementioned SAR data, indazole-3-carboxamide is a viable scaffold for the synthesis of compounds with PARP-1 inhibitory activity; however, the present results clearly suggest that its structural modification does not warrant that a desirable activity as a PARP-1 inhibitor will be realized. Therefore, our efforts were redirected to identify alternate novel NI-mimicking scaffolds that unlike indazole-3-carboxamide could be turned into highly active PARP-1 inhibitors.

To be able to shed some light on the molecular interactions of these inhibitors, we performed docking calculations on the most potent compound **5** using the crystal structure of a 2-substituted benzimidazole-4-carboxamide–PARP-1 complex (Figure 4). The hydrogen bonding pattern of the pharmacophoric amide group with Gly863 and Ser904 was similar to that observed for compound **2**. The π-stacking interaction of the indazole moiety was also similar to that of compound **2**. The 2,3-dioxindoline moiety binds into the AD site as inferred from its location at van der Waals interacting distances from the AD-binding residues such as Glu763, Asp766, Asn767, and Asp770. The C₂ carbonyl oxygen atom of the 2,3-dioxindoline moiety forms a water (HOH502)-mediated hydrogen bond with the backbone of Tyr896 (–C=O—H₂O—HN– Tyr896) whereas the C₃ carbonyl oxygen atom was found to be positioned within interacting distance (3.5 Å) from HOH475. The phenyl portion of the 2,3-dioxindoline is stabilized through pi-pi stacking interaction with

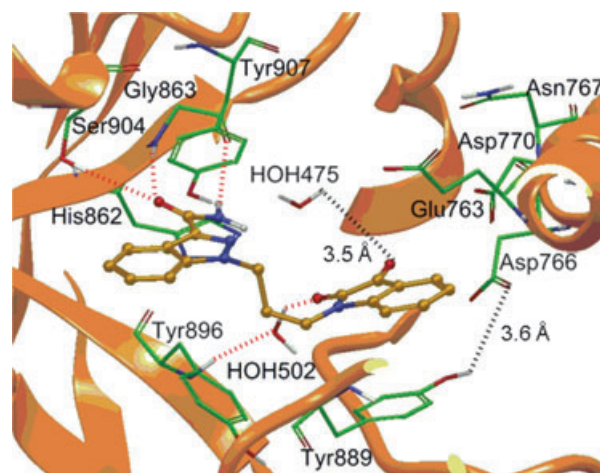


Figure 4: Standard precision-Glide predicted binding pose for compound **5** within the active site of poly(ADP-ribose)polymerase-1. Inhibitor is shown in ball and stick model, while the active site amino acids and water molecules are shown in stick model. Dotted red lines indicate hydrogen bonding interaction, whereas dotted black lines show the interacting distance. Color scheme is the same as in Figure 2.

Tyr889. It is interesting to note that in the crystal structure of PARP-1, the carboxylate group of Asp766 is located within interacting distance (3.6 Å) from the hydroxyl group of Tyr889 and this interaction seem to have implications in preserving the secondary structure and function of the enzyme (26,27). We speculate that the 2,3-dioxindoline ring may be involved in disrupting the aforementioned interaction by occupying the space between the side chains of Asp766 and Tyr889. The existence of no tolerance for substituents at the 5-position of the 2,3-dioxindoline moiety may be the result of steric hindrance with either the carboxylate group of Asp766 or the hydroxyl group of Tyr889.

Several studies have indicated that PARP-1 inhibitors participate in the regeneration of pancreatic β -islet cells and, as a result, they are able to delay or even reverse the progression of type 1 diabetes mellitus and some of its complications (7,8,28). A pharmacological agent that has been widely used to examine the beneficial effects of PARP-1 inhibitors in animal models of experimental diabetes has been STZ (11,12). STZ is a bacterial nitrosourea analog of D-glucose (2-deoxy-2-[3-methyl-3-nitrosoureido-D]glucopyranose) that is preferentially taken up by β -islet cells with the aid of the glucose transporter GLUT2 (11). STZ induces diabetes by promoting DNA breaks in insulin-producing pancreatic cells, mainly through alkylation and, to a lesser extent, by the generation of reactive oxygen species and reactive nitrogen species. These events will activate nuclear PARP-1 to synthesize large amounts of chromatin protein-bound ADP-ribose polymer from NAD⁺ and for altering the chromosomal structure to make the DNA-damaged site(s) accessible to repair enzymes (29). However, overactivation of PARP-1 will ultimately lead to the massive utilization of NAD⁺, a precursor of ATP, within pancreatic islet cells, and bring NAD⁺ and ATP contents to levels that are insufficient to meet the normal cellular energy requirements and are conducive to decreased function and necrotic cell death. An alternative view on the role of overactivation of PARP-1 as a determinant of cell death is that it initiates a nuclear signal that propagates to the mitochondrion and triggers the release of apoptosis-inducing factor. Apoptosis-inducing factor then shuttles from the mitochondrion to the nucleus, where it induces peripheral chromatin condensation, large-scale fragmentation of DNA, and, ultimately, apoptotic β -cell death (30). Irrespective of the mechanism of action of STZ in causing diabetes, this compound has been extensively utilized to induce experimental diabetes in rodents, especially mice and rats, in studies aimed at demonstrating the *in vivo* effectiveness of PARP-1 inhibitors and other chemical agents to attenuate diabetic hyperglycemia and hypoinsulinemia. Using the rat as an experimental model, it was possible to determine that an acute intraperitoneal (ip) treatment with STZ (60 mg/kg in citrate buffer pH 4.5) led to a significant increase in plasma glucose (by approximately 414%, $p < 0.001$ versus DMSO) and a significant decrease in plasma insulin (by 76%, $p < 0.001$ versus DMSO) (Table 2). In contrast, an ip pretreatment with compound **5**, given at doses equal to 0.7 and 1.4 mM/kg, led to a dramatic dose-related attenuation of the changes in plasma glucose (increases equal to only 85% and 8%, respectively, when compared to control animals receiving only DMSO, $p < 0.001$ versus STZ), an effect that was accentuated further at a dose of 2.1 mM/kg (decrease of 37% below the control value, $p < 0.001$ versus STZ). On the other hand, a pretreatment with the same doses of compound **5** counteracted the decrease in plasma insulin

Table 2: The effects of 3-AB and compound **5** on the plasma glucose and plasma insulin levels of rats made diabetic with streptozotocin (STZ)^{a,b,c}

Treatment	Plasma glucose, mg/dL	Plasma insulin, μ IU/mL
Physiological saline	79.42 \pm 4.65	0.491 \pm 0.015
Citrate buffer pH 4.5	78.18 \pm 5.42	0.482 \pm 0.013
DMSO	92.90 \pm 4.02	0.487 \pm 0.017
STZ	401.78 \pm 9.46 ^{***,†††}	0.113 \pm 0.007 ^{***,†††}
3-AB 2.1 mM/kg	87.38 \pm 1.76	0.457 \pm 0.003
5 1.4 mM/kg	98.05 \pm 3.38 ^{*†}	0.414 \pm 0.009
STZ + 3-AB 0.7 mM/kg	200.27 \pm 5.87 ^{***,†††,°°°}	0.191 \pm 0.006 ^{***,†††,°°°}
STZ + 3-AB 1.4 mM/kg	170.69 \pm 11.68 ^{***,†††,°°°}	0.257 \pm 0.014 ^{**††,°°°}
STZ + 3-AB 2.1 mM/kg	113.26 \pm 7.72 ^{**††,°°°}	0.303 \pm 0.022 ^{*†,°°°}
STZ + 5 0.7 mM/kg	171.60 \pm 4.20 ^{***,°°°,#}	0.206 \pm 0.007 ^{***,†††,°°°}
STZ + 5 1.4 mM/kg	99.91 \pm 6.00 ^{°°°,#}	0.298 \pm 0.008 ^{**††,°°°,#}
STZ + 5 2.1 mM/kg	58.88 \pm 3.08 ^{**°°°,††,###}	0.347 \pm 0.008 ^{*†,°°°,#}

^aValues for compound **5** were corrected for the contribution of the vehicle, DMSO, as determined from values for animals on physiological saline.

^bEach STZ + 3-AB treatment was compared with a STZ + **5** treatment at the same dose.

^cStatistical comparisons were vs. Citrate buffer pH 4.5 at ^{*} $p < 0.05$, ^{**} $p < 0.01$, ^{***} $p < 0.001$; vs. Physiological saline at [†] $p < 0.05$, ^{††} $p < 0.01$, ^{†††} $p < 0.001$; vs. STZ at ^{°°°} $p < 0.001$; vs. DMSO at ^{*} $p < 0.05$, ^{**} $p < 0.01$, ^{***} $p < 0.001$; vs. STZ + 3-AB at [#] $p < 0.05$, ^{##} $p < 0.01$, ^{###} $p < 0.001$

induced by STZ in a dose-related manner (decreases ranging from only 29–58%, $p < 0.001$ versus STZ). Moreover, a pretreatment with identical doses of 3-AB, a prototypical PARP-1 inhibitor, led to a weaker protective action against the hyperglycemia and hypoinsulinemia associated with STZ-induced diabetes than compound **5** (plasma glucose increases of 45-156%, plasma insulin decreases of 37-60% vs. normal (physiological saline) values, all differences at $p < 0.001$ versus STZ). The return of the insulin level to ~63% of control with the highest dose of 3-AB tested is in line with the value reported in the literature for this compound when given to rats 15 min before STZ (31). Furthermore, the present results for compounds **5** and 3-AB correlate well with their *in vitro* inhibitory potencies on PARP-1 (IC₅₀ = 6.80 μ M for compound **5**, IC₅₀ = 11.0 μ M for 3-AB). Table 2 summarizes the results for the *in vivo* evaluation of compounds **5** and 3-AB as antidiabetogenic agents. Because PARP-1, and probably some of its isoforms, is involved in the repair of damaged sites in DNA, it is likely that inhibition of the enzyme will result into accumulation of dsDNA breaks in normal tissues (13,32). Moreover, PARP inhibition may be associated with genomic instability because PARP has been described as the 'guardian angel protecting the genome' (33). However, it may also be noted that several PARP inhibitors are being advanced to Phase II/III oncology clinical trials.

Conclusions

We have synthesized a series of novel *N*-1-substituted indazole-3-carboxamide derivatives, demonstrating inhibitory activity toward PARP-1. In this series, compound **5** (IC₅₀ = 6.8 μ M) was found to be the most potent one. More importantly, compound **5** demonstrated a potent dose-related antidiabetogenic activity in an STZ-based animal model of experimental diabetes because it helped to reduce

the hyperglycemia and hypoinsulinemia induced by STZ at a greater extent than equivalent doses of 3-AB, a well-known PARP-1 inhibitor. In a continuing search for PARP-1 inhibitors with inhibitory potency greater than that of compound **5**, further synthetic and SAR work is presently ongoing and the results of which will be communicated in future.

Acknowledgments

Support to TT in the form of start-up funds and resources from the College of Pharmacy and Allied Health Professions, St. John's University, Queens, NY, are gratefully acknowledged. We thank Dr. Santosh Khedkar from Harvard Medical School and Dr. V. Hariprasad from Huntsman Cancer Institute for many helpful suggestions.

Conflict of Interest

The authors declare no competing interests.

References

- Otto H., Reche P.A., Bazan F., Dittmar K., Haag F., Koch-Nolte F. (2005) In silico characterization of the family of PARP-like poly(ADP-ribosyl)transferases (pARTs). *BMC Genomics*;6:139.
- Virag L., Szabo C. (2002) The therapeutic potential of poly(ADP-ribose) polymerase inhibitors. *Pharmacol Rev*;54:375–429.
- de Murcia G., Menissier de Murcia J. (1994) Poly(ADP-ribose) polymerase: a molecular nick-sensor. *Trends Biochem Sci*;19:172–176.
- Lautier D., Lagueux J., Thibodeau J., Menard L., Poirier G.G. (1993) Molecular and biochemical features of poly(ADP-ribose) metabolism. *Mol Cell Biochem*;122:171–193.
- Althaus F.R., Hofferer L., Kleczkowska H.E., Malanga M., Naegeli H., Panzeter C., Realini C. (1993) Histone shuttle driven by the automodification cycle of poly(ADP-ribose) polymerase. *Environ Mol Mutagen*;22:278–282.
- Poirier G.G., de Murcia G., Jongstrat-Bilen N.C., Mandel P. (1982) Poly(ADP-ribosylation) of polynucleosomes causes relaxation of chromatin structure. *Proc Natl Acad Sci USA*;79:3423–3427.
- Masiello P., Cubeddu T.L., Frosina G., Bergamini E. (1985) Protective effect of 3-aminobenzamide, an inhibitor of poly(ADP-ribose) synthetase, against streptozotocin-induced diabetes. *Diabetologia*;28:683–686.
- Masiello P., Novelli M., Fierabracci V., Bergamini E. (1990) Protection by 3-aminobenzamide and nicotinamide against streptozotocin-induced β -cell toxicity in vivo and in vitro. *Res Commun Chem Pathol Pharmacol*;69:17–32.
- Mabley J.G., Suarez-Pinzon W.L., Hasko G., Salzman A.L., Rabinovitch A., Kun E., Szabo C. (2001) Inhibition of poly(ADP-ribose) synthetase by gene disruption or inhibition with 5-iodo-6-amino-1,2-benzopyrone protects mice from multiple-low-dose-streptozotocin-induced diabetes. *Br J Pharmacol*;133:909–919.
- Charron M.J., Bonner-Weir S. (1999) Implicating PARP and NAD⁺ depletion in type I diabetes. *Nat Med*;5:269–270.
- Schnedl W.J., Ferber S., Johnson J.H., Newgard C.B. (1994) Streptozotocin transport and cytotoxicity. Specific enhancement in GLUT2-expressing cells. *Diabetes*;43:1326–1333.
- Yamamoto H., Uchigata Y., Okamoto H. (1981) Streptozotocin and alloxan induce DNA strand breaks and poly(ADP-ribose) synthetase in pancreatic islets. *Nature*;294:284–286.
- Woon E.C.Y., Threadgill M.D. (2005) Poly(ADP-ribose) polymerase inhibition – where now? *Curr Med Chem*;12:2373–2392.
- Ruf A., Mennissier D.M., de Murcia G., Schulz G.E. (1996) Structure of the catalytic fragment of poly(AD-ribose) polymerase from chicken. *Proc Natl Acad Sci USA*;93:7481–7485.
- Ruf A., Mennissier D.M., de Murcia G., Schulz G.E. (1998) Inhibitor and NAD⁺ binding to poly(ADP-ribose) polymerase as derived from crystal structures and homology modeling. *Biochemistry*;37:3893–3900.
- Saenz J., Mitchell M., Bahmanyar S., Stankovic N., Perry M., Craig-Woods B., Kline B., Yu S., Albizati K. (2007) Process development and scale-up of AG035029. *Org Process Res Dev*;11:30–38.
- Hunt K.W., Moreno D.A., Suiter N., Clark C.T., Kim G. (2009) Selective synthesis of 1-functionalized-alkyl-1*H*-indazoles. *Org Lett*;11:5054–5057.
- Kim J.-I., Jahng Y. (1995) Synthesis and biological activity of indazole-derived HMG-CoA reductase inhibitors. *Arch Pharm Res*;18:206–212.
- Begtrup M., Claramunt R.M., Elguero J. (1978) Azolides. Part 12. Carbon-13 nuclear magnetic resonance study of N-methyl and N-acetyl derivatives of azoles and benzazoles. *J Chem Soc Perkin Trans*;2:99–104.
- Palmer M.H., Findlay R.H., Kennedy S.M.F., McIntyre P.S. (1975) Reactivity of indazoles and benzotriazole towards N-methylation and analysis of the ¹H nuclear magnetic resonance spectra of indazoles and benzotriazoles. *J Chem Soc Perkin Trans*;1:1695–1700.
- Piozzi F., Ronchi A.U. (1963) Synthesis of substituted 3-indazole ketones. *Gazzetta Chimica Italiana*;93:3–14.
- Jorgensen W.L., Maxwell D., Tirado-Rives J. (1996) Development and testing of the OPLS all-atom force field on conformational energetics and properties of organic liquids. *J Am Chem Soc*;118:11225–11236.
- Purnell M.R., Whish W.J.D. (1980) Novel inhibitors of poly(ADP-ribose) synthetase. *Biochem J*;185:775–777.
- Banasik M., Komura H., Shimoyama M., Ueda K. (1992) Specific inhibitors of poly(ADP-ribose) synthetase and mono(ADP-ribosyl)transferase. *J Biol Chem*;267:1569–1575.
- Soriano F.G., Virag L., Jagtap P., Szabo E., Mabley J.G., Liaudet L., Marton A., Hoyt D.G., Murthy K.G.K., Salzman A.L., Southan G.J., Szabo C. (2001) Diabetic endothelial dysfunction: the role of poly(ADP-ribose) polymerase activation. *Nat Med*;7:108–113.
- Ishida J., Yamamoto H., Kido Y., Kamijo K., Murano K., Miyake H., Ohkubo M., Kinoshita T., Warizaya M., Iwashita A., Mihara K., Matsuoka N., Hattori K. (2006) Discovery of potent and selective PARP-1 and PARP-2 inhibitors: SBDD analysis via a combination of X-ray structural study and homology modeling. *Bioorg Med Chem*;14:1378–1390.
- Iwashita A., Hattori K., Yamamoto H., Ishida J., Kido Y., Kamijo K., Murano K., Miyake H., Kinoshita T., Warizaya M., Ohkubo

- M., Matsuoka N., Mutoh S. (2005) Discovery of quinazolinone and quinoxaline derivatives as potent and selective poly(ADP-ribose)polymerase-1/2 inhibitors. *FEBS Lett*;579:1389–1393.
28. Soriano F.G., Pacher P., Mabley J., Liaudet L., Szabo C. (2001) Rapid reversal of the diabetic endothelial dysfunction by pharmacological inhibition of poly(ADP-ribose) polymerase. *Circ Res*;89:684–691.
29. Bhat K.R., Benton B.J., Ray R. (2006) Poly (ADP-ribose) polymerase (PARP) is essential for sulfur mustard-induced DNA damage repair, but has no role in DNA ligase activation. *J Appl Toxicol*;26:452–457.
30. Hong S.J., Dawson T.M., Dawson V.L. (2004) Nuclear and mitochondrial conversations in cell death: PARP-1 and AIF signaling. *Trends Pharmacol Sci*;25:259–264.
31. Shima K., Hirota M., Sato M., Numoto S., Oshima I. (1987) Effect of poly(ADP-ribose) synthetase inhibitor administration to streptozotocin-induced diabetic rats on insulin and glucagon contents in their pancreas. *Diabetes Res Clin Pract*;3:135–142.
32. Meyer-Ficca M.L., Meyer R.G., Jacobson E.L., Jacobson M.K. (2005) Poly(ADP-ribose) polymerases: managing genome stability. *Int J Biochem Cell Biol*;37:920–926.
33. Tong W.-M., Cortes U., Wang Z.-Q. (2001) Poly(ADP-ribose) polymerases: a guardian angel protecting the genome and suppressing tumorigenesis. *Biochim Biophys Acta*;1552:27–37.

Supporting Information

Additional Supporting Information may be found in the online version of this article:

Figure S1. NOESY spectra for compound **3**.

Figure S2. NOESY spectra for compound **5**.

Table S1. PARP-1 inhibition data of *N*-1 substituted indazole-3-carboxamides.

Appendix S1. Preparation of *N*-(2-chloroethyl)-2,3-dioxindoline.

Appendix S2. Preparation of 1-(2-(2,3-dioxindolin-1-yl)ethyl)-1*H*-indazole-3-carboxamide.

Appendix S3. Preparation of *N*-(4-chlorobutyl)-2,3-dioxindoline.

Appendix S4. Preparation of 1-(4-(2,3-dioxindolin-1-yl)butyl)-1*H*-indazole-3-carboxamide.

Appendix S5. Preparation of 1-(3-(1,3-dioxoisindolin-2-yl)propyl)-1*H*-indazole-3-carboxamide.

Appendix S6. Preparation of 1-(3-(2,5-dioxopyrrolidin-1-yl)propyl)-1*H*-indazole-3-carboxamide.

Appendix S7. Preparation of 1-(oxiran-2-ylmethyl)-1*H*-indazole-3-carboxamide.

Appendix S8. Preparation of 1-(3-(2,3-dioxindolin-1-yl)-2-hydroxypropyl)-1*H*-indazole-3-carboxamide.

Appendix S9. Preparation of 1-(3-chloropropanoyl)-1*H*-indazole-3-carboxamide.

Appendix S10. Preparation of 1-(3-(2,3-dioxindolin-1-yl)propanoyl)-1*H*-indazole-3-carboxamide.

Please note: Wiley-Blackwell is not responsible for the content or functionality of any supporting materials supplied by the authors. Any queries (other than missing material) should be directed to the corresponding author for the article.